ЯДЕРНА ФІЗИКА
NUCLEAR PHYSICS

УДК 539.143+539.143.5 https://doi.org/10.15407/jnpae2018.04.326

Ali H. Taqi*, Ebtihal G. Khidher

Department of Physics, College of Science, Kirkuk University, Kirkuk, Iraq

*Corresponding author: alitaqi@uokirkuk.edu.iq; alitaqibayati@yahoo.com

GROUND AND TRANSITION PROPERTIES OF ^{40}Ca AND ^{48}Ca NUCLEI

Properties of the ground states and transitions in ^{40}Ca and ^{48}Ca nuclei are studied using the self-consistent Hartree - Fock and random phase approximation calculations with Skyrme-type interactions: KDE0, SLy4, LNS, RAPT and T6. The purpose of the paper is to obtain the best Skyrme-force parameterizations for description of the experimental data. All the calculated values were compared with the available data. The calculated binding energy per nucleon, charge root mean square, ground charge density distribution and transition strength distribution agree very well with the experimental data. The overall behavior of the calculated transition densities demonstrated the reliability of the method.

Keywords: charge density distribution, transition density, strength distribution, Skyrme - Hartree - Fock, random phase approximation.

1. Introduction

A nuclear many-body problem is generally difficult to solve exactly, as it arises in many branches of physics. Various approximate approaches exist to deal with such systems. Simple shell-model (SM) is based on the independent particle approximation, which ignores all correlation effects. It can be used in its simplest single-particle form to predicts or explains with some success properties of nuclei, in particular spin and parity of ground states, and to some extent their excited states as well.

The self-consistent mean-field SCMF theory in the quantum many-body problem is Hartree - Fock (HF) theory [1], assumes that nucleons move independently in a mean-field generated by the other nucleons of the atomic nucleus. SCMF calculation starts from an effective interaction between nucleon to drive the mean field and an SC interaction of single particle equations. The variation principle is applied to drive a set of coupled equation that yields minimized the value of ground-state energy as the best approximation which solved in a repetitive pattern. This type of models mainly include the relativistic mean field (RMF) [2] and the non-relativistic HF theories.

The main idea in non-relativistic HF approach is to calculated the NN interaction, such as the short finite range (Gongy-model) [3, 4] or zero range (Skyrme-model) [5 - 7] to describe ground state and low-energy excitation properties of finite nuclei and nuclear matter because these forces (Gongy and Skyrme) depend on about ten adjustable parameters that are fitted to reproduced relevant ground state properties of some nuclei.

In the case of closed shell and sub-shell nuclei, the simplest correlation beyond the HF can be described by breaking the HF core and raising a nucleon from below to above the Fermi level; then the collective excited states can be demonstrated as a linear combination of particle-hole (*ph*) states in truncated model space. In another language, this model is also expressed as the random phase approximation (RPA) theory.

Since the pioneering work of Brink and Vautherin [8], continuous efforts have been made to readjust the parameters of the Skyrme-type effective nucleon-nucleon interaction to better reproduce experimental data. Most of the set of parameters were obtained by the fitting of the HF results to experimental data on bulk properties of a few stable closed shell nuclei [9, 10]. Recently, were obtained by the fitting of HF results to the experimental data on the bulk properties of nuclei ranging from the β-stable nuclei to those near the proton and/or neutron drip lines [11 - 16]. M. Dutra et al. [17, 18] presented a detailed assessment of the ability of the 263 Skyrme interaction parameter sets in the literature to satisfy a series of criteria derived from macroscopic properties of nuclear matter in the vicinity of nuclear saturation density at zero temperature and their density dependence, derived by the liquid-drop model, in experiments with giant resonances and heavy-ion collisions.

Having a large number of the Skyrme-force parameterizations requires continuous search for the best in theoretically description of the nuclear structure, therefore in the present work, the nuclear structure of ^{40}Ca and ^{48}Ca nuclei has been studied in the framework of the self-consistent HF-RPA with

using Skyrme-type interactions KDE0, SLy4, LNS, RAPT and T6. The investigated interactions have different nuclear matter constraints, these sets of parameters may fit the ground-state properties (e.g. single-particles energies, binding energies, and radii) with some differences. But, more efforts need to assessment the calculated results of the excited properties.

2. Theory

The nuclear ground-state in HF calculation, is obtained by varying the nuclear Hamiltonian within the set of trial functions. Using the Wick's theorem, the HF energy can be obtained as in terms of the single-particle density ρ [19]

$$E^{HF} = \sum_{ij} \varepsilon_{ij} \rho_{ji} + \frac{1}{2} \sum_{ijkl} \rho_{ki} V_{ijkl} \rho_{lj} \tag{1}$$

In this work we adopt the following Skyrme-type effective NN interaction [16, 20]:

$$\begin{aligned} V_{12} &= t_0 \left(1 + x_0 P_\sigma\right) \delta(r) \\ &+ \frac{1}{2} t_1 \left(1 + x_1 P_\sigma\right) \left[\delta(r) k^2 + k'^2 \delta(r) \right] && \text{central term} \\ &+ t_2 \left(1 + x_2 P_\sigma\right) \vec{\mathrm{k}}' \cdot \delta(r) \vec{\mathrm{k}} && \text{non-local term} \\ &+ \frac{1}{6} t_3 \left(1 + x_3 P_\sigma\right) \rho^\alpha(R) \delta(r) && \text{density-dependent term} \\ &+ i W_0 \left(\vec{\sigma}_1 + \vec{\sigma}_2\right) \cdot \left[\vec{\mathrm{k}}' \cdot \delta(r) \vec{\mathrm{k}} \right], && \text{spin-orbit term} \end{aligned} \tag{2}$$

where $r = r_1 - r_2$, $R = \frac{(r_1 + r_2)}{2}$, $P_\sigma = (1 + \sigma_1.\sigma_2)/2$ is the spin-exchange operator, σ is the Pauli spin matrices and k' is the Hermitian conjugate of k (acting on the left) and it is given by

$$k = \frac{1}{2i} (\vec{\nabla}_1 - \vec{\nabla}_2), \; k' = -\frac{1}{2i} (\vec{\nabla}'_1 - \vec{\nabla}'_2),$$

where $t_0, t_1, t_2, t_3, x_0, x_1, x_2, x_3$ and W_0 are arbitrary adjustable parameters [21 - 23].

The ground proton, neutron and charge density distribution of a nucleus can be obtained using the Skyrme-HF radial wave functions $u(n\ell, r)$ [24, 25]

$$\rho_q(r) = \frac{1}{4\pi} \sum_{n\ell j} \eta_q (2j+1) \left| \frac{u(n\ell j, r)}{r} \right|^2. \tag{3}$$

Hence η_q = 0 or 1 for empty or fully occupied orbits respectively. The root-mean-square (rms) radii is defined as follows [26]:

$$\left\langle r_q^2 \right\rangle = \int_0^{R_{box}} \mathbf{r}^2 \rho_q(\mathbf{r}) \mathrm{d}^3\mathbf{r}. \tag{4}$$

The charge radius can be obtained approximately using the proton distribution

$$\left\langle r_{ch}^2 \right\rangle = \left\langle r_p^2 \right\rangle + \left\langle r \right\rangle_p^2 \tag{5}$$

with $\langle r \rangle_p = 0.8$ fm.

Beyond HF, the excited collective states of closed shell and subshell nuclei can be described by a linear combination of *ph* RPA states. Then the excited states $|\nu\rangle$ can be results from the action of excitation operator $Q_\nu^\dagger$ [19]

$$Q_\nu^\dagger = \sum_{mi} \left[X_{mi}^\nu a_m^\dagger a_i - Y_{mi}^\nu a_i^\dagger a_m \right], \tag{6}$$

where the label *m* represents particle states and *i* is for hole states. The *ph* RPA ground state is defined via the condition

$$Q_\nu |RPA\rangle = 0. \tag{7}$$

The probability of finding the particle-hole states $a_m^\dagger a_i |0\rangle$ and $a_i^\dagger a_m |0\rangle$ in the excited state $|\nu\rangle$ gives the amplitudes X_{mi} and Y_{im}

$$\begin{aligned} \langle 0 | a_i^\dagger a_m | \nu \rangle &\cong \langle HF | \left[a_i^\dagger a_m, Q_\nu^\dagger \right] | HF \rangle = X_{mi}^\nu, \\ \langle 0 | a_m^\dagger a_i | \nu \rangle &\cong \langle HF | \left[a_m^\dagger a_i, Q_\nu^\dagger \right] | HF \rangle = Y_{mi}^\nu. \end{aligned} \tag{8}$$

The *ph* RPA equations can be written in a compact matrix form

$$\begin{pmatrix} A & B \\ B^* & A^* \end{pmatrix} \begin{pmatrix} X^\nu \\ Y^\nu \end{pmatrix} = E_\nu \begin{pmatrix} 1 & 0 \\ 0 & -1 \end{pmatrix} \begin{pmatrix} X^\nu \\ Y^\nu \end{pmatrix} \tag{9}$$

with

$$A_{minj} = \langle HF | \left[a_i^\dagger a_m, \left[H, a_n^\dagger a_j \right] \right] | HF \rangle = (\varepsilon_m - \varepsilon_i) \delta_{mn} \delta_{ij} + V_{mjin}^{ph},$$

$$B_{minj} = -\left\langle HF\left|\left[a_i^\dagger a_m,\left[H,a_j^\dagger a_n\right]\right]\right|HF\right\rangle = V_{mnij}^{ph}. \quad (10)$$

ε_m is the single particle energy. In the J couples scheme, all the particle-particle pp residual interaction matrices should be in ph channel [6]

$$V_{mjin}^{ph} = -\sum_{J'}(2J'+1)\begin{Bmatrix} j_m & j_n & J' \\ j_i & j_j & J \end{Bmatrix} V_{mnij}^{pp}. \quad (11)$$

The residual interaction can be built from the self-consistent Skyrme-HF energy density functional

$$V_{mjin}^{ph} = \frac{\delta^2 E^{HF}}{\delta\rho_{mi}\delta\rho_{nj}}. \quad (12)$$

The strength function is defined by the transition operators as follows

$$S(E) = \sum_{\nu}\left|\left\langle \nu\left\|\hat{F}_J\right\|0\right\rangle\right|^2 \delta(E-E_\nu), \quad (13)$$

where $\hat{F}_J$ is the nuclear multipole operator between the RPA ground $|0\rangle$ and excited states $|\nu\rangle$ with the corresponding excitation energy E_ν. For plotting purpose, the strength functions is approximated as follows:

$$S(E) = \sum_{\nu}\left|\left\langle \nu\left\|\hat{F}_J\right\|0\right\rangle\right|^2 \rho_\Gamma(E-E_\nu), \quad (14)$$

where the Lorentzian function is defined as in the following:

$$\rho_\Gamma(E-E_\nu) = \frac{\Gamma}{2\pi}\frac{1}{(E-E_\nu)^2+(\Gamma/2)^2} \quad (15)$$

with Γ is the smearing parameter.

The radial transition density of state $|\nu\rangle$ is defined as follows [27]:

$$\delta\rho_\nu(r) = \frac{1}{\sqrt{2J+1}}\sum_{mi}\left[X_{mi}^{(\nu)}+Y_{mi}^{(\nu)}\right]\left\langle m\left\|Y_J\right\|i\right\rangle \frac{u_m(r)u_i(r)}{r^2}, \quad (16)$$

where X and Y are RPA amplitudes. The isoscalar IS (T = 0) and isovector IV (T = 1) densities defined

$$\delta\rho_\nu^{(IS)}(r) \equiv \delta\rho_{\nu_n}(r)+\delta\rho_{\nu_p}(r), \quad (17)$$

$$\delta\rho_\nu^{(IV)}(r) \equiv \delta\rho_{\nu_n}(r)-\delta\rho_{\nu_p}(r). \quad (18)$$

The reduced matrix elements of the spherical harmonic Y_J is expressed as [28]

$$\left\langle m\left\|Y_J\right\|i\right\rangle = (-1)^{j_m+\frac{1}{2}}\sqrt{\frac{(2j_m+1)(2j_i+1)(2J+1)}{4\pi}}\begin{pmatrix} j_m & J & j_i \\ 1/2 & 0 & -1/2 \end{pmatrix}\frac{1}{2}\left[1+(-1)^{\ell_m+J+\ell_i}\right]. \quad (19)$$

3. Results and Discussion

In this study, the equations of the static HF were solved by using the Numerov method with the radial mesh of size h = 0.1 fm within a model space based on Skyrme-type interactions KDE0 [29], SLy4 [13], LNS [30], RAPT [31] and T6 [32].

The HF calculations have been investigated for ^{40}Ca and ^{48}Ca nuclei, including the ground state properties: binding energy, root mean square radii and the charge density distributions, were compared with the available experimental data. The theoretical binding energies per nucleon calculated using 5-type Skyrme interactions for the investigated nuclei are listed in Tables 1 and 2 respectively with the corresponding experimental data [33]. The results are in good agreement with available experimental data.

Table 1. **Binding energies per nucleon B/E, and rms radii of neutron, proton, and charge of ^{40}Ca, calculated using the KDE0, LNS, SLy4, RTAP and T6 Skyrme interaction sets**

Force	E/A, MeV	$\langle r_n^2\rangle^{1/2}$, fm	$\langle r_p^2\rangle^{1/2}$, fm	$\langle r_{ch}^2\rangle^{1/2}$, fm
Exp.	-8.55 [33]			3.48 [34]
KDE0	-8.94	3.33	3.38	3.47
SLy4	-8.61	3.37	3.41	3.51
LNS	-8.69	3.22	3.28	3.37
RAPT	-8.59	3.37	3.41	3.50
T6	-8.27	3.38	3.42	3.51

Table 2. **Binding energies per nucleon B/E, and rms radii of neutron, proton, and charge of ^{48}Ca, calculated using the KDE0, LNS, SLy4, RTAP and T6 Skyrme interaction sets**

Force	E/A, MeV	$\langle r_n^2 \rangle^{1/2}$, fm	$\langle r_p^2 \rangle^{1/2}$, fm	$\langle r_{ch}^2 \rangle^{1/2}$, fm
Exp.	-8.67 [33]			3.47 [34]
KDE0	-9.10	3.57	3.42	3.51
SLy4	-8.71	3.61	3.46	3.55
LNS	-8.77	3.46	3.30	3.40
RAPT	-8.70	3.60	3.45	3.54
T6	-8.41	3.61	3.45	3.55

The calculations with the KDE0, LNS, SLy4, RTAP and T6-type Skyrme parameterizations of the neutron, proton and charge root mean square (rms) radii for ^{40}Ca along with the experimental data [34] are shown in Tables 1 and 2 respectively. Our results show that the calculated charge rms radii are close to the experimental data with a slight difference by type of Skyrme parameterizations. Our results are comparable with the earlier studies with SI, SII, SIII, BLV1 and SL1 in ref. [9].

The nuclear charge density is the most helpful notice for considering the nuclear structure. It gives us a picture of the internal structure of nuclei. Figs. 1 and 2 display the calculated HF charge distribution for ^{40}Ca and ^{48}Ca nuclei, respectively with 5-type Skyrme parameterizations. Most of the interactions have an agreement with the experimental data [34] at the surface and interior regions. The calculated results of the interaction LNS have a deviation from data at the surface region for the investigated nuclei.

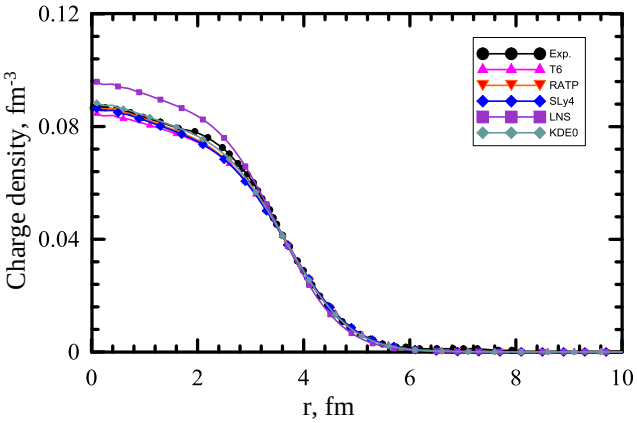

Fig. 1. Charge density distribution for ^{40}Ca calculated with the KDE0, LNS, SLy4, RTAP and T6 Skyrme interactions and compared with experimental data [34]. (See color Figure on the journal website.)

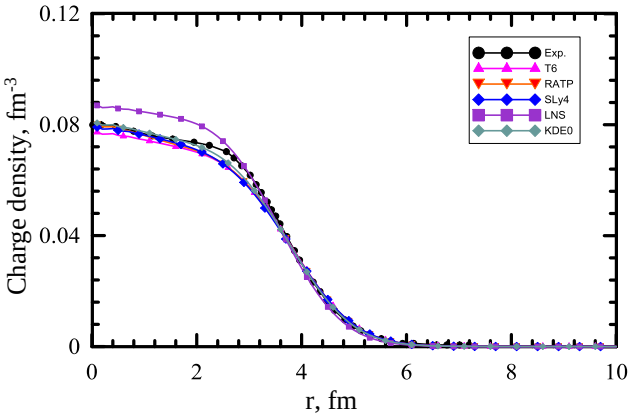

Fig. 2. Charge density distribution for ^{48}Ca calculated with the KDE0, LNS, SLy4, RTAP and T6 Skyrme interactions and compared with experimental data [34]. (See color Figure on the journal website.)

The code skyrme_rpa [27, 35] has been used to perform the full self-consistent RPA matrix diagonalization within the selected model space. The *ph* configurations between all possible occupied and unoccupied states were restricted by the cut-off energy equal to 50 MeV.

The giant resonance region from 9.5 MeV < E_x < < 40 MeV in ^{48}Ca was studied with inelastic scattering of 240 MeV α particles at small angles, including 0°. Close to 100 % of the the isoscalar giant monopole resonance (ISGMR) ($E0$), isoscalar giant dipole resonance ISGDR ($E1$), and isoscalar giant quadrupole resonance (ISGQR) ($E2$) strengths have been located between 9.5 and 40 MeV in ^{48}Ca [36]. To study the effect of neutron-proton asymmetry, a comparison with the available data for ^{40}Ca [37 - 39], as well as with the results obtained within the HF-RPA, was carried out in ref. [36]. The ISGMR was found at somewhat higher energy in ^{48}Ca than in ^{40}Ca, whereas self-consistent HF-RPA calculations obtained using the SGII, KDE0, SKM*, and SK255 Skyrme interactions predict a centroid energy in this neutron-rich Ca isotope lower than in ^{40}Ca [36].

In this work, the excitation properties of ^{40}Ca and ^{48}Ca nuclei including the strength distributions and transition densities were calculated in the long wavelength limit by considering the KDE0, LNS, SLy4, RTAP and T6-type Skyrme parameterizations for the three most important giant resonance: the ISGMR, the isoscalar giant quadrupole resonance

(ISGQR), and the IVGDR. The interest of the transition densities relies on the fact that their spatial shape reveal the nature of the excitations: volume or surface type, IS or IV etc.

The strength distributions (fraction of EWSR) of isoscalar monopole E0 and quadrupole E2, and isovector dipole $E1$ photo absorption cross section (mb) are shown in Figs. 3 and 4 for the studied nuclei. Lorenzian smearing Γ of 3 MeV width was used in the calculation, and compared with the experimental data [36, 38, 40]. Most interactions work best and agree with data concerning centroid energy, widths and (smooth) profiles of strength. For the ISGMR, fragmented structure seen in some interactions.

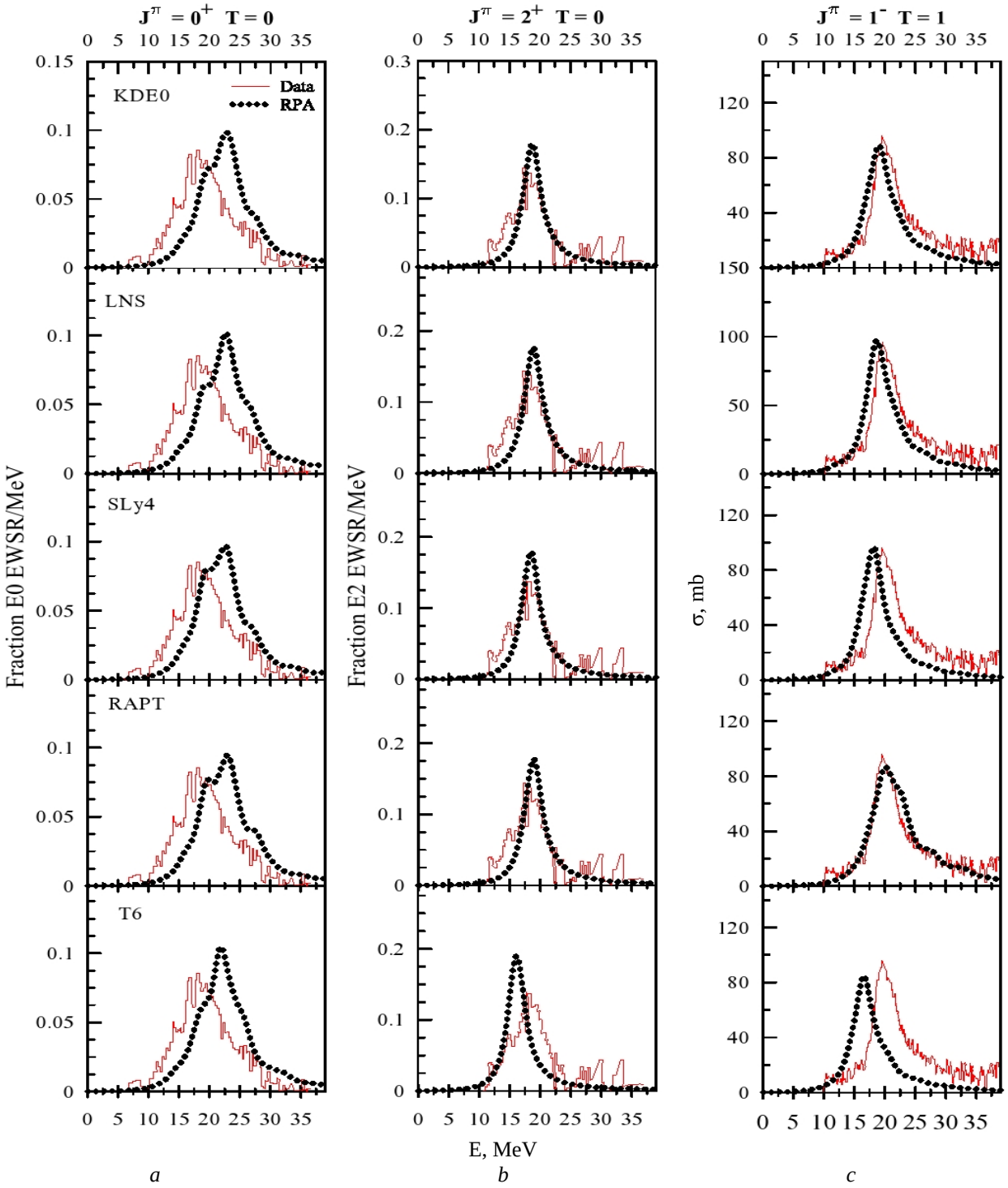

Fig. 3. Our calculations of the strength distribution for the fraction of EWSR: *a* – isoscalar monopole (E0); *b* – quadrupole (E2); *c* – photo absorption dipole cross section (E1) in ^{40}Ca, obtained using the KDE0, LNS, SLy4, RTAP and T6 Skyrme interactions. A Lorenzian smearing Γ of 3 MeV was used in the calculation. Experimental data are from [38] for ISGMR and ISGQR and [40] for IVGDR, are shown as red-solid lines. (See color Figure on the journal website.)

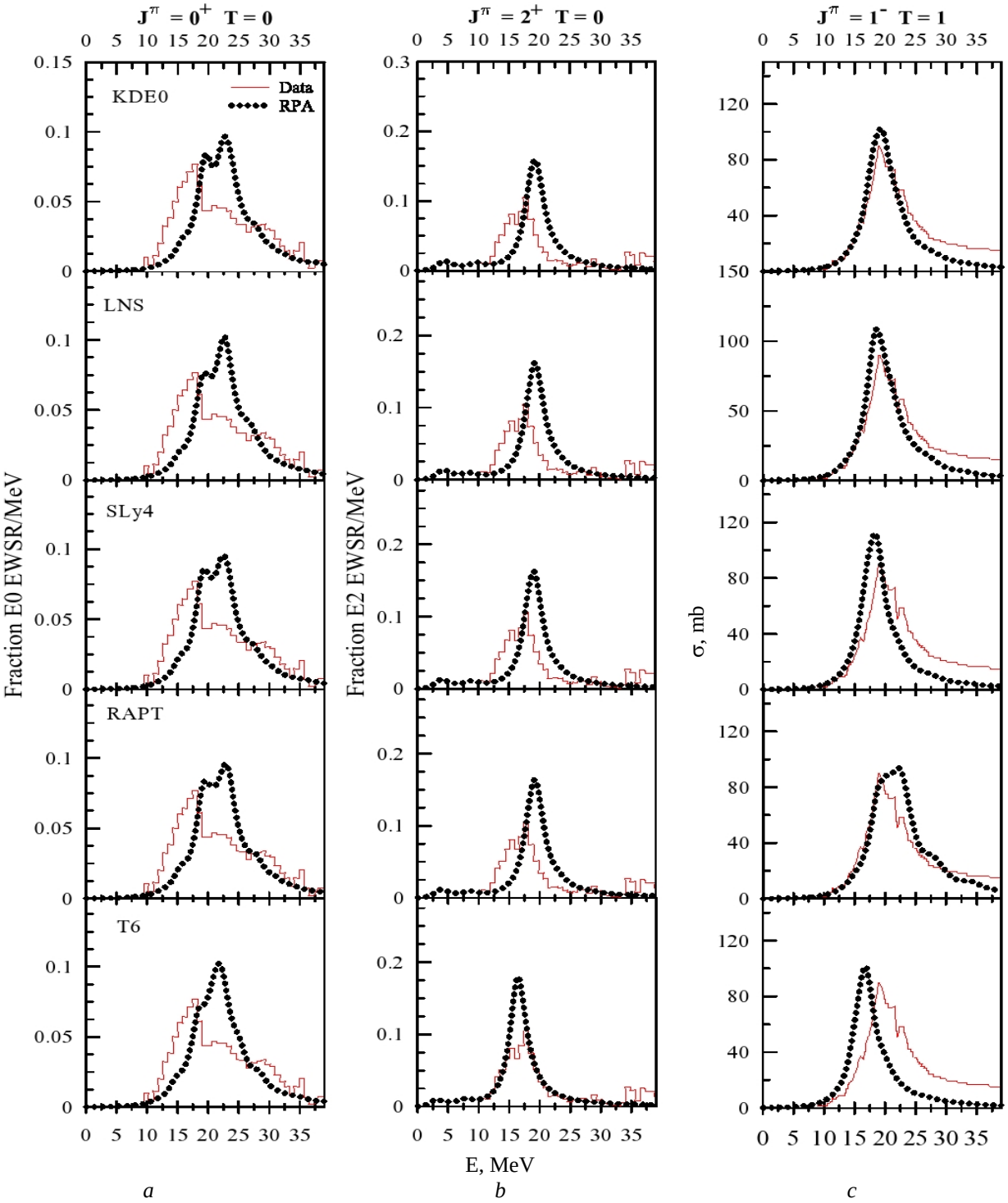

Fig. 4. Our calculations of the strength distribution for the fraction of EWSR: *a* – isoscalar monopole (E0); *b* – quadrupole (E2); *c* – photo absorption dipole cross section (E1) in 48Ca, obtained using the KDE0, LNS, SLy4, RTAP and T6 Skyrme interactions. A Lorenzian smearing Γ of 3 MeV was used in the calculation. Experimental data are from [36] for ISGMR and ISGQR and [40] for IVGDR, are shown as red-solid lines. (See color Figure on the journal website.)

In Figs. 5 and 6 the calculated transition densities of proton and neutron for ^{40}Ca and ^{48}Ca are presented as a function of the radial coordinate of the states using KDE0, LNS, SLy4, RTAP and T6-type interactions for the ISGMR, IVGDR, and ISGQR. In the ISGMR mode, the surface of the nucleus is confirmed for the centroid energy range 19 - 25 MeV for ^{40}Ca and ^{48}Ca. Clearly, protons and neutrons are oscillated in the same trend, in all cases, the surface has a dominant IS character. The same behavior is illustrated for peak energy in ISGQR, i.e, the IS character of the surface of the nucleus is confirmed, for the energy range 15 - 22 MeV for ^{40}Ca and 13 - 18 MeV for ^{48}Ca.

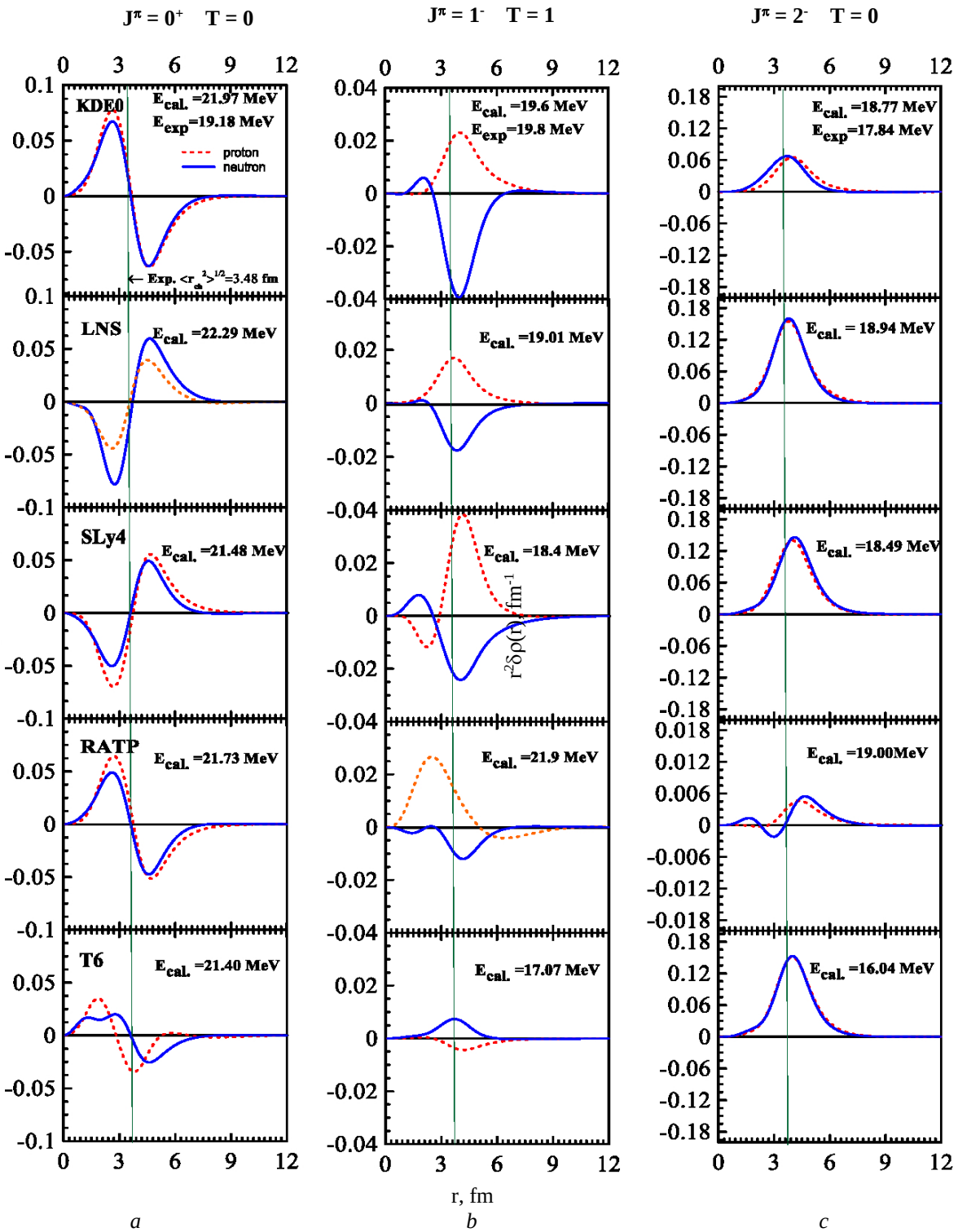

Fig. 5. Transition densities of proton and neutron for ^{40}Ca: *a* – Isoscalar monopole; *b* – isovector dipole; *c* – isoscalar quadrupole. The HF-RPA calculations were done with KDE0, LNS, SLy4, RTAP and T6 Skyrme interaction. (See color Figure on the journal website.)

The total transition in IVGDR mode is dominated by IV component for the main strength peaks around 17 - 23 MeV for ^{40}Ca and 16 - 24 MeV for ^{48}Ca. Obviously, both protons and neutrons contribute to the transition and oscillate in opposite directions.

In our results, we do not have pigmy giant resonance (PGR) because the GDR mode, is IS and involves the motion of mainly internal nucleons, the PDR is IS behavior more than IV and includes the motion of the external nucleons, which are mainly neutrons. In our case, the number of neutrons in the studied nuclei does not exceed the number of protons too much.

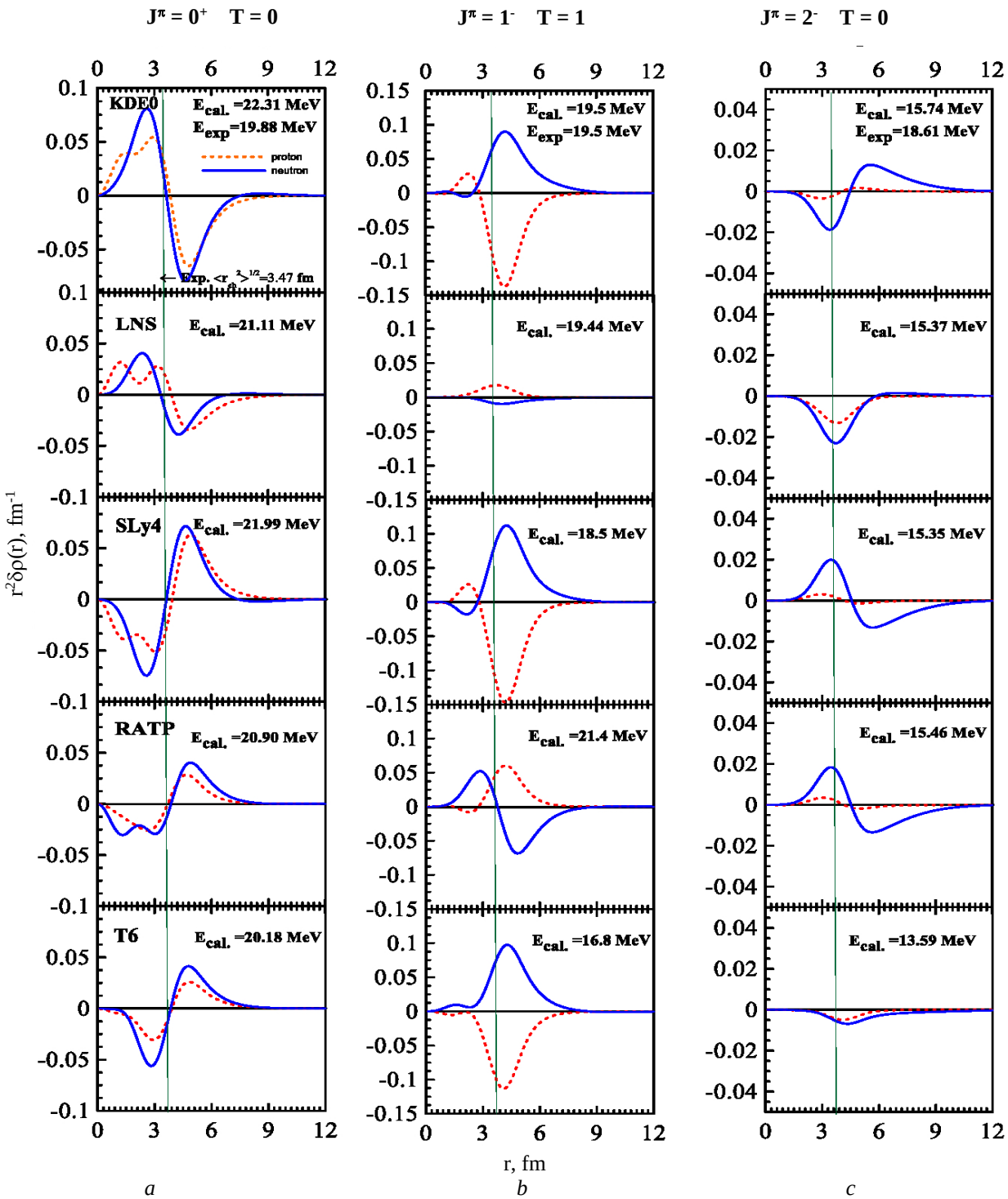

Fig. 6. Transition densities of proton and neutron for ^{48}Ca: *a* – isoscalar monopole; *b* - isovector dipole; *c* – isoscalar quadrupole. The HF-RPA calculations were done with KDE0, LNS, SLy4, RTAP and T6 Skyrme interaction. (See color Figure on the journal website.)

4. Conclusions

The ground and transition properties of the even-even nuclei ^{40}Ca and ^{48}Ca were studied in the framework of the self-consistent HF-RPA using 5-type Skyrme interaction parameterization. Our results give a reasonable description of the experimental data. In conclusion, the calculated results are in very good agreement with the available experimental data for the most type of Skyrme interactions. The overall behavior of the calculated transition densities demonstrated the reliability of the method. The used method can be readily used in giving a good description and understanding of the nuclear structure of the investigated nuclei, this serving as a sign or indication of to the validity and success of the self-consistent HF and the *ph* RPA for such even-even nuclei, especially for *pf*-shell nuclei.

REFERENCES

1. P. Klüpfel, P.G. Reinhard. Self-consistent mean-field models for nuclear structure and dynamics. Int. J. Mod Phys. E 16(4) (2007) 1009.
2. P. Ring. Relativistic mean field theory in finite nuclei. Prog. Part. Nucl. Phys. 37 (1996) 193.
3. T. Abe et al. Monte Carlo Shell Model for ab initio nuclear structure. EPJ Web of Conferences 66 (2014) 02001.
4. S. Péru, M. Martini. Mean field based calculations with the Gogny force: Some theoretical tools to explore the nuclear structure. Eur. Phys. J. A 50(5) (2014) 1.
5. J.W. Negele. The mean-field theory of nuclear structure and dynamics. Rev. Mod. Phys. 54 (1982) 913.
6. J.R. Stone, P.-G. Reinhard. The Skyrme interaction in finite nuclei and nuclear matter. Prog. Part. Nucl. Phys. 58 (2007) 587.
7. B.K. Agrawal, S. Shlomo, V. Kim Au. Determination of the parameters of a Skyrme type effective interaction using the simulated annealing approach. Phys. Rev. C 72 (2005) 014310.
8. D. Vautherin, D.M. Brink. Hartree-Fock Calculations with Skyrme's Interaction. I. Spherical Nuclei. Phys. Rev. C 5 (1972) 626.
9. K.-F. Liu et al. Skyrme-Landau parameterization of effective interactions. (I). Hartree-Fock ground states. Nucl. Phys. A 534 (1991) 1.
10. K.-F. Liu, H. Luo, Zh. Ma. Skyrme-Landau parametrization of effective interactions. (II). Self-consistent description of giant multipole resonances. Nucl. Phys. A 534 (1991) 25.
11. P.G. Reinhard, H. Flocard. Nuclear effective forces and isotope shifts. Nucl. Phys. A 584 (1995) 467.
12. E. Chabanat et al. A Skyrme parametrization from subnuclear to neutron star densities. Nucl. Phys. A 627 (1997) 710.
13. E. Chabanat et al. A Skyrme parametrization from subnuclear to neutron star densities. Part II. Nuclei far from stabilities. Nucl. Phys. A 635 (1998) 231.
14. B.A. Brown. New Skyrme interaction for normal and exotic nuclei. Phys. Rev. C 58 (1998) 220.
15. P.-G. Reinhard et al. Shape coexistence and the effective nucleon-nucleon interaction. Phys. Rev. C 60 (1999) 014316.
16. M. Bender, P.H. Heenen, P.G. Reinhard. Self-consistent mean-field models for nuclear structure. Rev. Mod. Phys. 75 (2003) 121.
17. M. Dutra et al. Skyrme interaction and nuclear matter constraints. Phys. Rev. C 85 (2012) 035201.
18. M. Dutra et al. Relativistic mean-field hadronic models under nuclear matter constraints. Phys. Rev. C 90 (2014) 055203.
19. P. Ring, P. Schuk. *The Nuclear Many-Body Problem* (Springer-Verlag, Berlin, 1980).
20. J.R. Stone, P.-G. Reinhard. The Skyrme interaction in finite nuclei and nuclear matter. Prog. Part. Nucl. Phys. 58(2) (2007) 587.
21. S. Goriely et al. Hartree-Fock mass formulas and extrapolation to new mass data. Phys. Rev. C 66 (2002) 024326.
22. P. Klüpfel et al. Variations on a theme by Skyrme: A systematic study of adjustments of model parameters. Phys. Rev. C 79 (2009) 034310.
23. M. Kortelainen et al. Nuclear energy density optimization. Phys. Rev. C 82 (2010) 024313.
24. N. Antonov, P.E. Hodgson, I. Zh. Petkov. *Nucleon Momentum and Density Distribution in Nuclei* (London: Oxford University Press, 1988).
25. Ali H. Taqi. A visual Fortran 90 program for the two-particle or two-hole excitations of nuclei: The PPRPA program. SoftwareX 5 (2016) 51.
26. C. Titin-Schnaider, Ph. Quentin. Coulomb exchange contribution in nuclear Hartree-Fock calculations. Phys. Lett. B 49(5) (1974) 397.
27. G. Colò et al. Self-consistent RPA calculations with Skyrme-type interactions: The skyrme_rpa program. Comp. Phys. Comm. 184(1) (2013) 142.
28. P.J. Brussaard, P.W. Glaudemans. *Shell Model Applications in Nuclear Spectroscopy* (North-Holland: Amsterdam, 1977).
29. M.N. Harakeh, A.M. Van Der Woude. *Giant resonances: Fundamental High-Frequency Modes of Nuclear Excitations* (London: Oxford University Press, 2001).
30. L.G. Cao et al. From Brueckner approach to Skyrme-type energy density functional. Phys. Rev. C 73 (2006) 014313.
31. M. Rayet et al. Nuclear force and the properties of matter at high temperature and density. Astronomy & Astrophysics 116 (1982) 183.
32. F. Tondeur et al. Static nuclear properties and the parametrisation of Skyrme forces. Nucl. Phys. A 420(2) (1984) 297.
33. National Nuclear Data Center (NNDC). http://www.nndc.bnl.gov
34. H. De Vries, C.W. De Jager, C. De Vries. Nuclear charge-density-distribution parameters from elastic electron scattering. Atomic Data and Nuclear Data Table 36 (1987) 495.
35. Ali H. Taqi, S. Ali Mohamed. Self-consistent Hartree-Fock RPA calculations in ^{208}Pb. Indian J. Phys. 92(1) (2017) 69.
36. Y.-W. Lui et al. Isoscalar giant resonances in ^{48}Ca. Phys. Rev. C 83 (2011) 044327.
37. D.H. Youngblood et al. Isoscalar $E0$ strength between 6 and 11 MeV in ^{40}Ca. Phys. Rev. C 68 (2003) 057303.
38. D.H. Youngblood, Y.-W. Lui, H.L. Clark. Isoscalar E0, E1, and E2 strength in ^{40}Ca. Phys. Rev. C 63 (2001) 067301.
39. D.H. Youngblood, Y.-W. Lui, H.L. Clark. Giant monopole resonance strength in ^{40}Ca. Phys. Rev. C 55 (1997) 2811.
40. V.A. Erokhova et al. Giant resonance in nuclei of calcium isotopes. Izv. Ross. Akad. Nauk, Ser. Fiz. 67 (2003) 1479 [Bull. Russ. Acad. Sci. Phys. 67 (2003) 1636].

Алі Х. Такі*, Ебтіхал Г. Кідхер

Кафедра фізики, коледж науки, університет Кіркук, Кіркук, Ірак

Відповідальний автор: alitaqi@uokirkuk.edu.iq; alitaqibayati@yahoo.com

ВЛАСТИВОСТІ ОСНОВНИХ СТАНІВ ТА ПЕРЕХОДІВ В ЯДРАХ ^{40}Ca І ^{48}Ca

Властивості основних станів та переходів в ядрах ^{40}Ca та ^{48}Ca було вивчено з використанням самоузгоджених обчислень у наближенні Хартрі - Фока та випадкових фаз із взаємодіями типу Скірма: KDE0, SLy4, LNS, RAPT та T6. Метою дослідження було отримання параметрів сил Скірма, що найкраще описують експериментальні дані. Усі розраховані значення порівнювалися з наявними даними. Розрахована енергія зв'язку на нуклон, зарядовий радіус, розподіл густини основного стану і розподіл імовірностей переходів добре узгоджуються з експериментальними даними. Загальна поведінка розрахованих імовірностей переходів показала надійність застосованого наближення.

Ключові слова: розподіл густини заряду, імовірність переходів, розподіл імовірностей, сили Скірма, наближення Хартрі - Фока, наближення випадкових фаз.

Али Х. Таки*, Эбтихал Г. Кидхер

Кафедра физики, колледж науки, университет Киркук, Киркук, Ирак

Ответственный автор: alitaqi@uokirkuk.edu.iq; alitaqibayati@yahoo.com

СВОЙСТВА ОСНОВНЫХ СОСТОЯНИЙ И ПЕРЕХОДОВ В ЯДРАХ ^{40}Ca И ^{48}Ca

Свойства основных состояний и переходов в ядрах ^{40}Ca и ^{48}Ca были изучены с использованием самосогласованных расчетов в приближении Хартри - Фока и случайных фаз с взаимодействием типа Скирма: KDE0, SLy4, LNS, RAPT и T6. Целью исследования было получение параметров сил Скирма, которые наилучшим образом описывают экспериментальные данные. Все вычисленные значения сравнивались с существующими данными. Рассчитанная энергия связи на нуклон, зарядовый радиус, распределение плотности основного состояния и распределение вероятностей переходов хорошо согласуются с экспериментальными данными. Общее поведение рассчитанных вероятностей переходов показало надежность использованного приближения.

Ключевые слова: распределение плотности заряда, вероятность перехода, распределение вероятностей, силы Скирма, приближение Хартри - Фока, приближение случайных фаз.

Надійшла 11.04.2018
Received 11.04.2018